Constructal design of elliptic tubes cooled by natural convection

Ahmed Waheed Mustafa, Jaafar Ahmed Zahi

College of Engineering, Mechanical Engineering Department, Al-Nahrain University, Baghdad, Iraq.

Abstract
The optimal spacing between elliptic tubes cooled by free convection is studied experimentally and numerically. A row of isothermal elliptic tubes are installed in a fixed volume and the spacing between them is selected according to the constructal theory (Bejan's theory). In this theory the spacing between the tubes is chosen such that the heat transfer density is maximized. A finite volume method is employed to solve the governing equations; SIMPLE algorithm with collocated grid is utilized for coupling between velocity and pressure. For the numerical study, the range of Rayleigh number is ($10^3 \leq Ra \leq 10^5$), the range of the axis ratio of the tubes is ($0 \leq \varepsilon \leq 0.5$), and the working fluid is air (Pr =0.71). Eexperimental study is also carried out in order to demonstrate the existence of the optimal spacing. The experimental Rayleigh number is (3.5×10^4) and the axis ratio of the elliptic tube is $\varepsilon = 0.25$. The numerical results show that the optimal spacing decreases as Rayleigh number increases for all axis ratios, and the maximum density of heat transfer increases as the Raleigh number increases for all axis ratios and the highest value occurs at axis ratio (ε =0) (flat plate) while the lowest value occurs at (ε =0.5) (circular tube). The results also show that the optimal spacing is unchanged with the axis ratio at constant Rayleigh number. The agreement between the experimental and numerical heat transfer density is qualitative.

Keywords: Constructal theory; Optimal spacing; Elliptic tubes; Natural convection.

1. Introduction
In heat transfer, constructal theory (Bejan's theory) is used to generate the flow configuration by optimizing the heat transfer density under (space) volume constraint. Constructal theory states that the flow configuration is free to morph in the follow-up of maximal global performance (objective function) under global constraints, Bejan and Lorente [1]. By depending on constructal theory, the optimal spacing between plates and cylinders cooled by natural convection can be found, in each geometry, the total volume is fixed and the objective is to maximize the overall thermal conductance between the tubes. Bejan [2], found the optimal spacing between vertical plates installed in a fixed volume by using the intersecting of asymptotes method. The study was employed for isothermal vertical plates cooled by natural convection. He found that the optimal spacing was proportional to the Raliegh number to the power of (-1/4). Bejan et al. [3] carried out a numerical and experimental study of how to choose the spacing among horizontal cylinders installed in a fixed volume cooled by laminar free convection. They

maximized the total density of heat transfer between the assembly and the ambient. The Numerical and experimental simulations cover the Rayleigh number range of $10^4 \leq Ra \leq 10^7$ and Pr = 0.72. In this study Bejan developed fundamental conclusions for the selection of the optimal spacing among horizontal cylinders in an assembly of fixed volume. More significant fundamentally was the conclusion that the maximum thermal conductance and optimal spacing can be expressed in compact dimensionless relations. Ledezma and Bejan [4], investigated numerically and experimentally the free convection from staggered vertical plates installed in fixed space. They maximized the density of heat transfer and they considered three degrees of freedom; the horizontal spacing between adjacent columns, the stagger between columns and the plate dimensions. Numerical and experimental simulations cover the Rayleigh number range of $10^3 \leq Ra \leq 10^6$, and the working fluid was air with Pr=0.72. The conclusion demonstrated numerically and experimentally that it was possible to optimize geometrically the internal architecture of a fixed volume such that its global thermal resistance was minimized. Da Silva and Bejan [5], studied numerically the free convection in vertical converging or diverging channel with optimized for density of heat transfer. They considered three degrees of freedom: the distribution of heat on the wall, wall to wall spacing, and the angle between the two walls. The optimization was performed in the range of ($10^5 \leq Ra \leq 10^7$) and (Pr=0.7). The walls were partially heated either at top of the channel or at the bottom of the channel. They proved that the density of heat transfer increased by putting the unheated part at the upper sections. They also showed that the best angle among the walls was almost zero when Ra number was high. Da Silva and Bejan [6], designed numerically a multi-scale plates geometry cooled by free convection by using constructal theory. They maximized the density of heat transfer rate. They put small plates in the unused heat transfer area between the large plates. They used finite element method to discretize the governing equation in the range of Rayleigh number of $10^5 \leq Ra \leq 10^8$, and Pr= 0.7. They showed that the density of heat transfer increased by putting the small plates between the large plates. Da Silva et al. [7] studied the free convection from discrete heat sources placed in vertical open channel with the constructal theory. They considered two cases, the first was single heat source under variable size, and the second was heat sources with fixed size. They applied the constructal theory to maximize the thermal conductance between the cold air and the discrete heat sources or to minimize the hot spot on the hot sources. Rayleigh number was in the range of ($10^2 \leq Ra \leq 10^4$) and Pr=0.7. They showed that for case one the thermal performance can be maximized as the heat source not covering the entire wall at Ra=102 and 103. When the intensity of inflow increased the optimal size of the heat source was equal the wall height. They also showed that for the second case best position of the heat sources changed with increasing of Rayleigh number and the optimal position of the last heat source was near the exit plane. Bello-Ochende and Bejan, [8] designed numerically a multi-scale cylinders geometry cooled by free convection by using constructal theory. They maximized the density of heat transfer rate. They put small cylinders in the unused heat transfer area between the large cylinders. They used finite element method to discretize the governing equation in the range of Rayleigh number of ($10^5 \leq Ra \leq 10^8$), and (Pr= 0.7). They showed that the density of heat transfer increased by putting the small cylinders between the large cylinders. Page et al., [9] investigated numerically the free convection from single scale rotating cylinders. They used the constructal theory to maximize the density of heat transfer rate. The range of Rayleigh number was ($10^1 \leq Ra \leq 10^4$), the range of rotating speed was ($0 \leq \tilde{\omega}_o \leq 10$), and the fluid was air (Pr=0.7). They found that the optimized spacing decreases as Rayleigh number increases and the heat transfer density increases. Page et al. [10] investigated numerically the free convection from multi-scales rotating cylinders. They used constructal theory in order to find the optimal arrangement of the geometry. The range of Rayleigh number was ($10^2 \leq Ra \leq 10^4$), the range of rotating speed was ($0 \leq \tilde{\omega}_o \leq 10$), and the fluid was air (Pr=0.7). Small cylinders were put in the unused regions of heat transfer. They found that there were no effects of the rotating cylinders on heat transfer density in compare with the stationary cylinders except at high speeds of rotation. They also found that the optimal spacing maximum density of heat transfer decreased as the rotation speed increased at each Rayleigh number. It is obvious from the literature that there is no attempt to find the optimal spacing between elliptic tubes cooled by natural convection with constructal theory, so that the present study uses the constructal theory to find the spacing numerically.

2. Mathematical model

Consider a row of elliptic tubes installed in a fixed volume per unit depth ($d L$) as shown in Figure 1. The major axis of the elliptic tube is ($a = d/2$), the minor axis of the tube is (b). The axis ratio is defined as (ε

=b/d). The tubes are maintained at constant wall (hot) temperature of(T_w), the ambient temperature is maintained at constant temperature of (T_∞). The objective is to find the number of tubes or the tube – to – tube spacing (s) for different axis ratio (ε) in order to maximize the heat transfer density. Therefore there are two degrees of freedom in this geometry, the first is the spacing (s) and the second is the axis ratio (ε). The dimensionless governing equations for steady, laminar, and incompressible flow with Boussinesq approximation for the density in the buoyancy term can be written as ; Zhang et al. [11]

$$\left(\frac{\partial U}{\partial X} + \frac{\partial V}{\partial Y}\right) = 0 \tag{1}$$

$$\left(U\frac{\partial U}{\partial X} + V\frac{\partial U}{\partial Y}\right) = -\frac{\partial P}{\partial X} + \left(\frac{Pr}{Ra}\right)^{1/2}\left(\frac{\partial^2 U}{\partial X^2} + \frac{\partial^2 U}{\partial Y^2}\right) \tag{2}$$

$$\left(U\frac{\partial V}{\partial X} + V\frac{\partial V}{\partial Y}\right) = -\frac{\partial P}{\partial X} + \left(\frac{Pr}{Ra}\right)^{1/2}\left(\frac{\partial^2 V}{\partial X^2} + \frac{\partial^2 V}{\partial Y^2}\right) + T \tag{3}$$

$$\left(U\frac{\partial T}{\partial X} + V\frac{\partial T}{\partial Y}\right) = \frac{1}{(Ra\,Pr)^{\frac{1}{2}}}\left(\frac{\partial^2 T}{\partial X^2} + \frac{\partial^2 T}{\partial Y^2}\right) \tag{4}$$

The non-dimensionalised variables and groups used are:
Coordinates $X = \frac{x}{d}$, $Y = \frac{y}{d}$, Horizontal velocity $U = \frac{u}{\left(\frac{\propto}{d}\right)(Ra\,Pr)^{\frac{1}{2}}}$, Vertical velocity $V = \frac{v}{\left(\frac{\propto}{d}\right)(Ra\,Pr)^{\frac{1}{2}}}$,
Pressure $P = \frac{Pd^2}{\propto^2 \rho\,Ra\,Pr}$, Temperature $T = \frac{t - T_\infty}{T_w - T_\infty}$, Prandtl number $Pr = \frac{v}{\propto}$, Rayleigh number $Ra = \frac{g\beta\,d^3\,(T_w - T_\infty)}{\propto v}$.

Since the flow is symmetrical between the tubes, only half of the flow channel between two tubes can be used to find the spacing in the numerical solution. Half of the flow channel is shown in Figure 2. The total height of the channel is (H_u+D+ H_d), the upstream height (H_u) and downstream (H_d) are added to avoid the applying of incorrect velocity and temperature at the inlet and outlet of the channel, these extension (H_u, H_d) are selected according to accuracy tests as shown later.
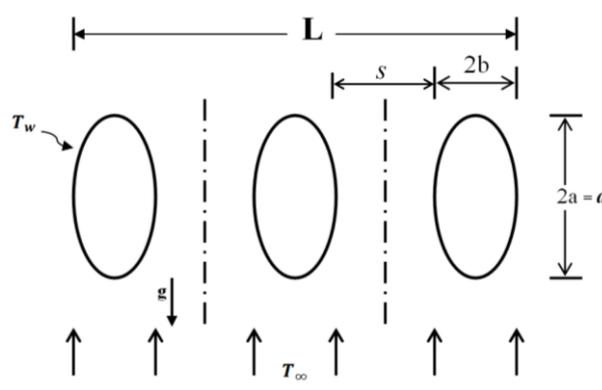
Figure 1. Physical geometry of the present problem.

The flow and thermal dimensionless boundary conditions on the half channel are shown in Figure 2 and can be summarized as;
Tube surfaces ($H_u \leq Y \leq D$) (no slip and no penetration and constant wall temperature U=V=0, T=1).
Channel inlet $\left(0 \leq X \leq \left(\frac{S}{2} + \varepsilon\right)\right)\left(U = \frac{\partial V}{\partial Y} = 0, T = 0, P = 0\right).$
Channel exit $\left(0 \leq X \leq \left(\frac{S}{2} + \varepsilon\right)\right)\left(\frac{\partial(U,V,T)}{\partial Y} = 0, P = 0\right).$
Left and right sides of the upstream section ($0 \leq Y \leq H_u$) (free slip and no penetration $U = \frac{\partial V}{\partial X} = 0, \frac{\partial P}{\partial X} = 0, \frac{\partial T}{\partial X} = 0$).

<u>Left side of the downstream section</u> $(H_u + D \leq Y \leq H_u + D + H_d)$ (free slip and no penetration $U = \frac{\partial V}{\partial X} = 0, \frac{\partial P}{\partial X} = 0, \frac{\partial T}{\partial X} = 0)$.

<u>Right side of the downstream section</u> $(H_u + D \leq Y \leq H_u + D + H_d)$ (zero stress $\frac{\partial(V,U)}{\partial X} = 0, \frac{\partial P}{\partial X} = 0, \frac{\partial T}{\partial X} = 0)$.

The right side of the downstream boundary condition is applied to permit fluid to enter the domain horizontally in order to avoid the vertical acceleration which generated by chimney effects, Bello-Ochende and Bejan [8].
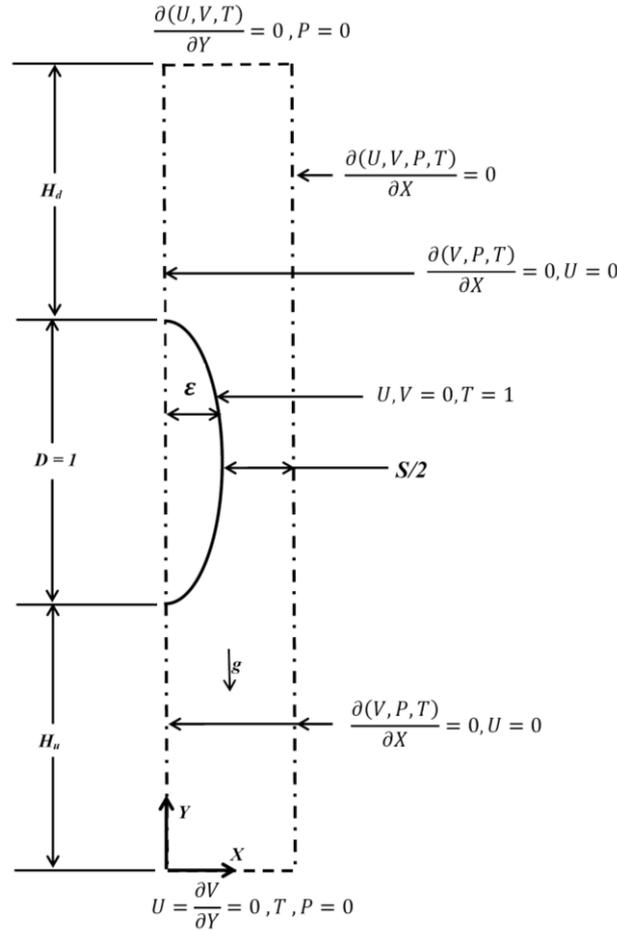
Figure 2. Dimensionless boundary conditions on the flow channel.

3. Optimization of heat transfer (maximum heat transfer density)

The spacing between the tubes is to be chosen such that the heat transfer density (objective function) is maximum. The heat transfer density is defined as the heat transfer rate per unit volume and given as;

$$q''' = \frac{q}{V} = \frac{q}{(s+2b)dW} = \frac{q'}{(s+2b)d} \tag{5}$$

where q' = Total heat transfer rate from one tube per unit width.
The heat transfer density can be written in non-dimensional form as;

$$Q = \frac{q'd^2}{k\,(T_w - T_\infty)(s+2b)d} \tag{6}$$

$$Q = \frac{-\left(\int_0^d k\frac{\partial T}{\partial x} dy\right)d}{k(T_w - T_\infty)(s+2b)} = \frac{-\int_0^1 \frac{\partial T}{\partial X} dY}{(S+2\varepsilon)} \tag{7}$$

where; Q: Non-dimensional heat transfer density, s: Dimensional Spacing between the tubes, S: Non-dimensional Spacing between the tubes.
The objective function (heat transfer density) subjected to the constraint that the total volume per unit width is fixed.

$$\therefore (d\ L) = \text{Constant} \tag{8}$$

4. Numerical procedure, grid independence test, and validation
A FORTRAN program is written to solve the algebraic equations which obtained by the finite volume method. The general transport equation is firstly transformed to curvilinear coordinates and the convective term is discretized by hybrid scheme while the diffusion term is discretized by second order central scheme. For coupling between the pressure and velocity SIMPLE algorithm is employed. To prevent the oscillation in the pressure field the interpolation method of Rhie and Chow, [12] is used. The system of algebraic equation is solved by TDMA and the convergence criterion of iteration is that the total imbalance in the source term in the pressure correction equation becomes less than 10-4. Further computational details can be found in Rhie and Chow [12]. The grid independence test is performed for three grids for configuration at which (Ra=104, ε =0.1, and S=0.3). The grid independence test showed that the increasing of the grid size decreases the error percentage, and the minimum error is at 50×50 control volumes per (D). So this grid size is used and adopted in all results. Gird independence test is illustrated in Table 1. To apply the correct velocity and temperature at the inlet and outlet of the channel, the upstream extension (Hu) is added at the inlet of the channel and downstream extension (Hd) is added at the outlet of the channel. It is observed from the Table 2 for (Ra=10^5, ε =0.25, and S=0.1) that the increasing in downstream extension to (Hd=2) and keeping the upstream at (Hu =0.5) leads to reduce the error in the heat transfer density to 2.5%. Based on this test the value of (Hu=0.5) and (Hd=2) have been depended in all numerical results. The numerical results are validated by comparing the results of (Sopt) with the numerical results of Da Silva and Bejan [5] for natural convection between vertical isothermal plates ($\varepsilon = 0$) and with Bello-Ochende and Bejan [8] for natural convection between isothermal cylinders ($\varepsilon = 0.5$). Both comparisons are carried out at (Ra =10^5). Good agreement can be shown in Table 3 for both cases. The procedure of the programming is investigated on flow chart at Figure 3.

Table 1. Grid independence test for the case (Ra =10^4, ε=0.1 and S= 0.3)

Number of control volumes per $D_\circ$	Q	Error%
30 × 30	30.94532	-
40 × 40	31.41611	0.69
50 × 50	31.21666	0.63

Table 2. Downstream extension test for the case (Ra =10^5, $\varepsilon = 0.25$, $H_u = 0.5$ and S =0.1).

H_d	Q	Error%
0.5	31.27484	-
1	32.50780	3.94
1.5	33.41908	2.8
2	34.26481	2.5

Table 3. Comparison of the numerical results for (S_{opt}) with the previous results for case (Ra =10^5, ε=0 and ε =0.5).

Flat Plate (ε= 0)	
Da Silva and Bejan [5]	Present
0.129	0.13
Circular Tube (ε= 0.5)	
Bello − Ochende and Bejan [8[	Present
0.104	0.12
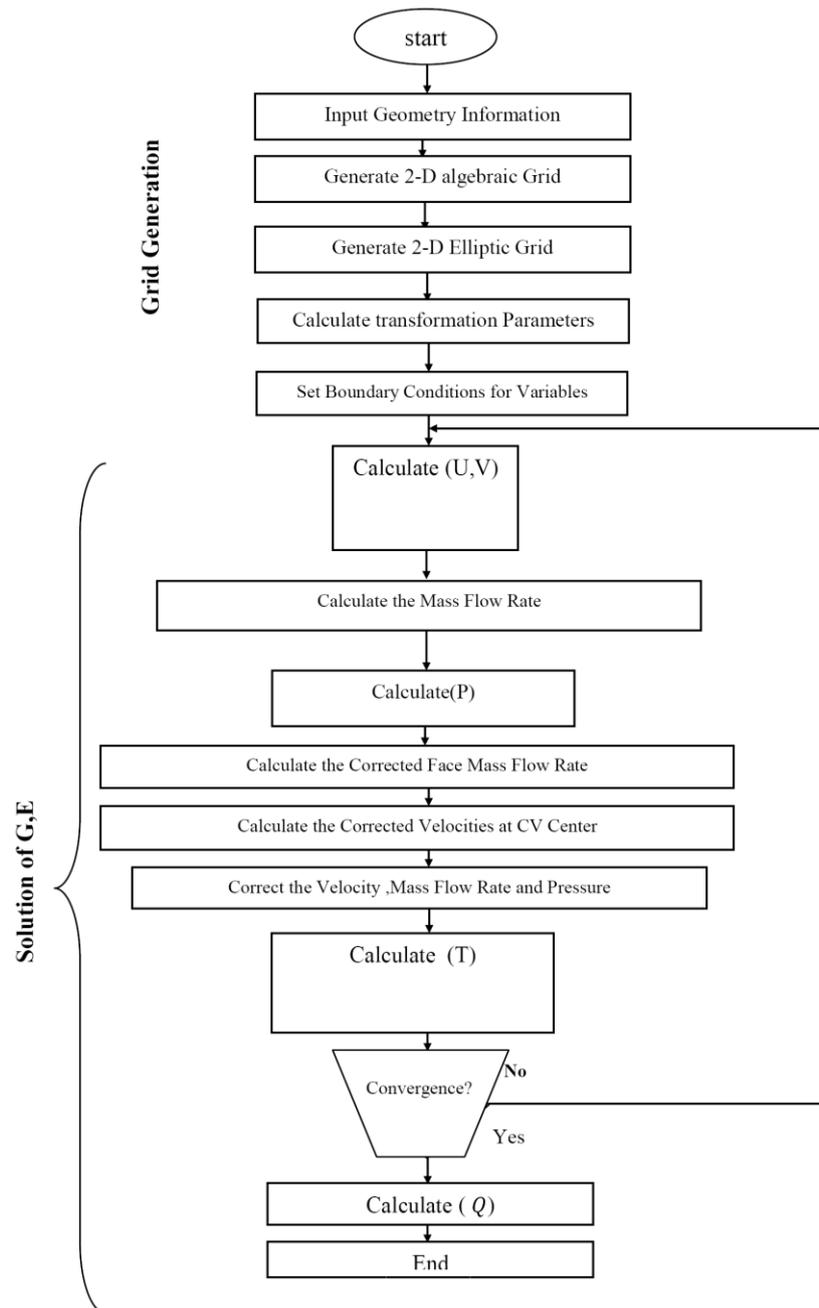
Figure 3. Program flow chart.

5. Experimental apparatus and procedure

In order to find the optimal spacing between elliptic tubes experimentally a rows of heated elliptic tubes are installed in a fixed volume. Figure 4 shows the main parts of the rows used in the experiments. In all experiments the tubes are placed is fixed volume of (d=24 mm, L=69 mm, and w=155 mm). Three rows of elliptic tubes are manufactured from circular copper tubes for the experiments, the first row consists of 5 tubes, the second row consists of 4-tubes, and the third row consists of 3 tubes. The spacing between the tubes in the first row is (2.25 mm) which corresponds to (S=s/d= 0.039), the spacing between the tubes in the second row is (7 mm) which corresponds to (S=s/d=0.291), and the spacing between the tubes in the third row is (10.5 mm) which corresponds to (S=s/d=0.4375). The three assemblies of tubes are shown in Figure 5. In order to minimize the heat loss from the tube ends, the tubes are held between two vertical wooden walls as shown in plate (1). The assembly is placed in open top and bottom ends Perspex enclosure of height (1m) and cross section of (0.42m x 0.42m), to minimize the radiation losses the walls of the enclosure are covered with aluminum foils. A two elliptic aluminum rollers are made

with major axis of (a=12 mm) and minor axis of (b=6 mm) in order to form an elliptic tube of axis ratio of (ε=0.25). A circular copper tube is pushed inside the rollers and pulled from the other side to form the elliptic tube. To heat the tubes a cartridge heaters of 9 mm diameter and 300 Watts are installed inside the tubes. These heaters are placed concentrically inside the tubes by using two rings at each ends of the tubes, the gaps between the heaters and the tubes are filled with the magnesium oxide powder. The heaters are connected in parallel and supplied by variable transformer which used to control the electrical power. The current and the voltage are measured by using (Digital Clamp Meter UNI-T UT200A with accuracy $\pm$ (1.5%+5)) as shown in plates. The uniform in temperature on the tube wall is firstly checked by six T-type thermocouples (calibrated with a mixture of ice and water) which located on the positions shown in Figure 6. The tube is then rotated to change the position of the thermocouples. The temperature is practically uniform when the maximum difference in the six locations about (0.3°C). The temperatures (T_{w1}) and (T_{w2}) are measured in the mid-plane of the row, as steady state is attained the maximum temperature registered is (T_{w1}) which used in the calculation of heat transfer density as shown later.

The first run (experiment for the row of 5 tubes) is started by supplying the electric power to the heaters to heat the elliptic tube. After the steady state attained which takes about 6-8 hours, the temperatures (T_{w1}, T_{w2} T_∞), the current, and the voltage are recorded. The steady state is attained when the percentage change in T_w, voltage, and current is less than 0.6%, 0.2% and 0.2% respectively.

The second experiment (4 tubes) and the third experiment (3 tubes) are conducted by adjusting the current in order to obtain the same temperature of the first experiment (T_{w1}) to make all the three experiments conducted at the same Rayleigh number.

(a)   (b)   (c)
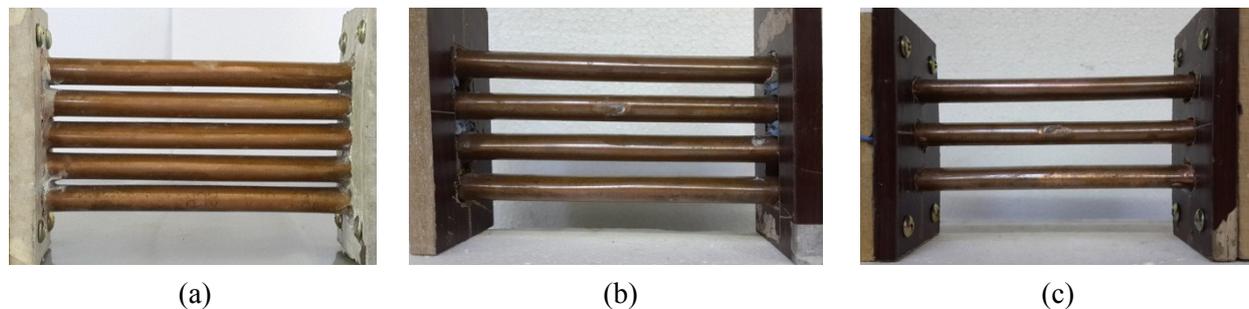
Figure 4. (a) Case 1 top view for five elliptic tubes, (b) Case 2 top view for five elliptic tubes, (c) Case 3 top view for five elliptic tubes.
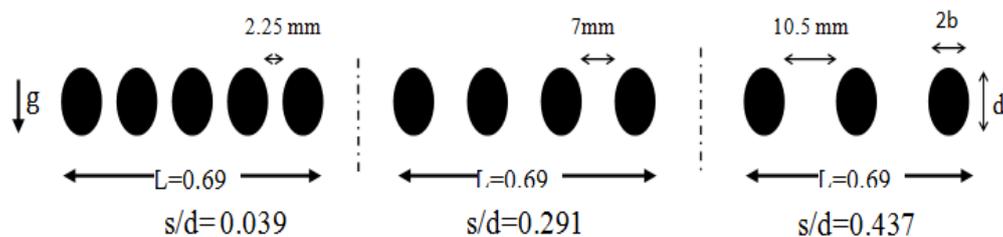
Figure 5. Details of main parts of the rows used in the experimental apparatus.
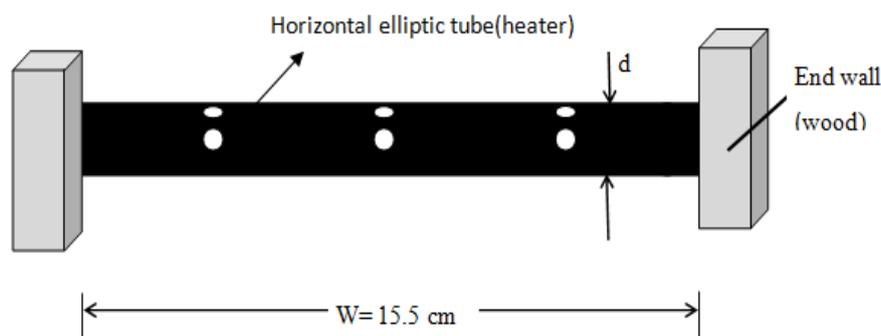
Figure 6. Position of the thermocouples on the elliptic tube

6. Numerical results

The numerical results are presented in this section for temperature contours, optimal spacing and density of heat transfer for different values of tube axis ratio ($0 \leq \varepsilon \leq 0.5$). The rang of Rayleigh is ($10^3 \leq Ra \leq 10^5$) and the working fluid is air with (Pr = 0.71).

Figure 7 show the temperature contour as a function of the spacing between the tubes (S) for (Ra=10^3) and axis ratio (ε=0.1) with noted that the gradation number (1) represented the red region of maximum heat temperature T_w and the gradation (0) represented the blue region of minimum heat temperature T_∞ according to the relation ($T = \frac{t - T_\infty}{T_w - T_\infty}$). For small spacing ($S \leq 0.25$) the downstream region is occupied by hot fluid at temperature same as the wall temperature (red region), this is due to that the small spacing between the tubes prevents the cold air to flow downstream and the air there still hot (overworked fluid). As the spacing between the tubes increases ($S \geq 0.25$) the downstream temperature begins to decrease and become less than the wall temperature and this is clear from appearance of the (orange, yellow and green) regions. At some spacing the thermal boundary layers from both sides are merged at the downstream region (the channel is fitted with the convective flow body), at this spacing the heat transfer density becomes maximum and the spacing represents the optimal spacing, in this case (S_{opt}= 0.41). Further increasing in spacing between the tubes leads to a cold fluid region to appear in the downstream as seen in the blue region (underworked fluid) for ($S \geq 1$), this large spacing permits to the ambient (cold) fluid to flow downstream and leads to decrease the heat transfer density since the thermal conductance between the tubes decreased.

As Rayleigh number increases to (Ra =10^4) same behavior of the temperature contour to that of ($Ra = 10^3$)as can be observed in Figure 8 except that the optimum spacing here becomes smaller, note that ($S_{opt} = 0.41$ at Ra =10^3) while ($S_{opt} = 0.22$ at Ra =10^4), so as Rayleigh number increases,the optimal spacing decreases because the thermal boundary layer thickness decreases with increasing of Rayleigh number, this is also obvious from the temperature contour for (Ra =10^5) in Figure 9 in which the optimal spacing is $S_{opt} = 0.12$ while the optimal spacing for (Ra =10^4) is (0.22).

Figures 10-12 illustrate the temperature contours at ($\varepsilon = 0.25$) and for Rayleigh numbers ($10^3, 10^4 and 10^5$), respectively. The temperature contours are similar to that of ($\varepsilon = 0.1$) at the same Rayleigh number.

Figures 13 and 14 show the dimensionless heat transfer density as a function of the spacing at different Rayleigh numbers and for (ε =0.1, 0.25) respectively. These figures show that there is optimal spacing for each Rayleigh number. At this value of spacing the heat transfer density reaches its maximum value (tops of the curves).

Figure 15 shows the optimal spacing (S_{opt}) versus Rayleigh number at various axis ratio ($\varepsilon = 0.1,0.25$, and 0.5), it is interesting to note that the optimal spacing decreases as Rayleigh number increases for all values of (ε), as mentioned above the increasing of Rayleigh number reduces the thermal boundary layer thickness and thus the optimal spacing decreased.

Figure 16 shows the maximum heat transfer density versus Rayleigh number at various axis ratio (ε), it can be noted that the maximum heat transfer density increases as Rayleigh number increases for all values of (ε), the increasing of Rayleigh number leads to increase the buoyancy force and thus increase the maximum heat transfer density. It also can be seen that the highest value of the maximum heat transfer density occurs at (ε =0, flat plate) and decreases as the axis ratio increases until reaches the lowest value at (ε =0.5, circular plate). This can be explained as the axis ratio increases (the curvature of the surface increases) the temperature gradient near the wall deceases and thus the maximum heat transfer density decreases.

Figure 17 shows the optimal spacing versus the axis ratio of the tube at different Rayleigh numbers. The optimal spacing is almost constant for all values of the axis ratio. Since the optimal spacing is nearly constant for all (ε), the number of tubes installed in the same volume must be reduced as the axis ratio increases.
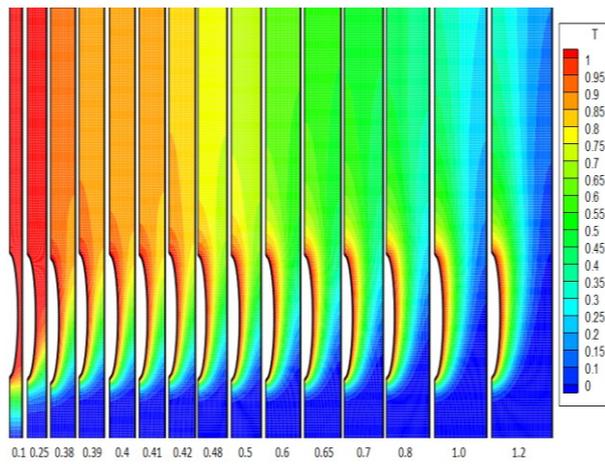
Figure 7. Temperature contour with various spacing between the tubes for (Ra=10^3, $Pr = 0.7$ and axis ratio ε = 0.1).
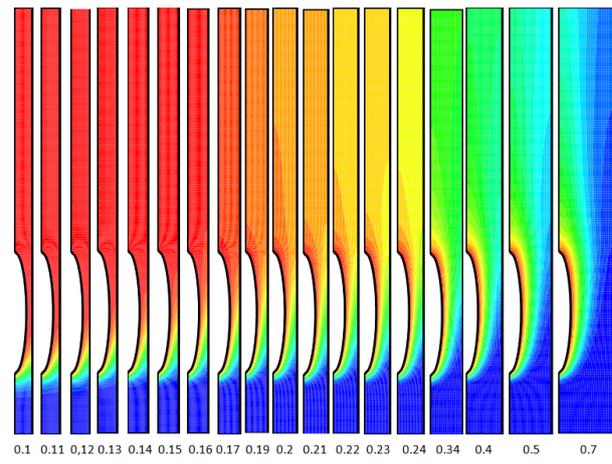
Figure 8. Temperature contour with various spacing between the tubes for (Ra=10^4, $Pr = 0.7$ and axis ratio ε= 0.1).
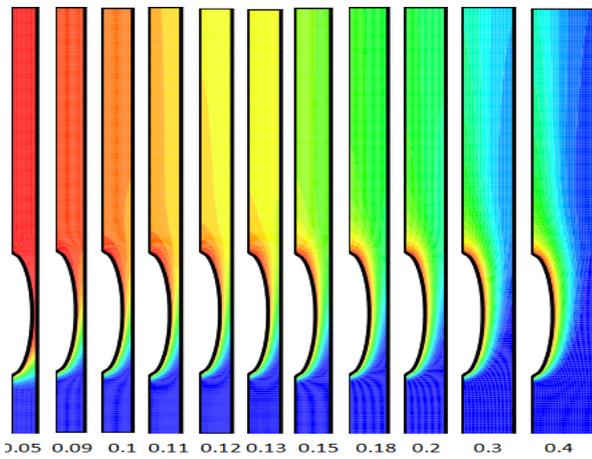
Figure 9. Temperature contour with various spacing between the tubes for (Ra=10^5, $Pr = 0.7$ and axis ratio ε= 0.1).
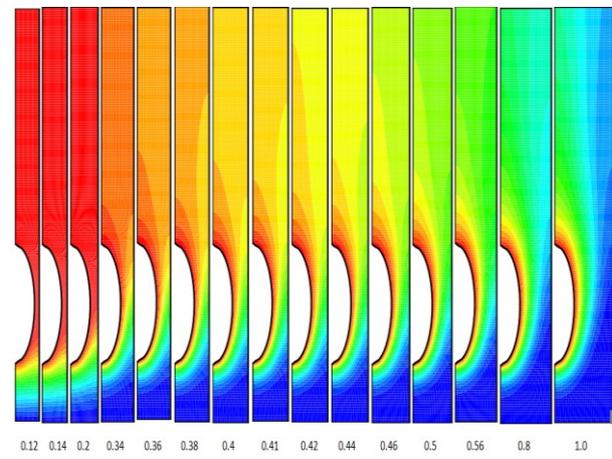
Figure 10. Temperature contour with various spacing between the tubes for (Ra=10^3, $Pr = 0.7$ and axis ratio ε= 0.25).
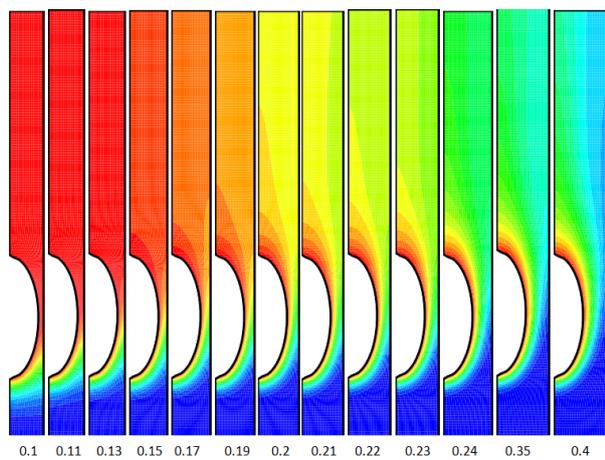
Figure 11. Temperature contour with various spacing between the tubes for (Ra=10^4, $Pr = 0.7$ and axis ratio ε= 0.25).
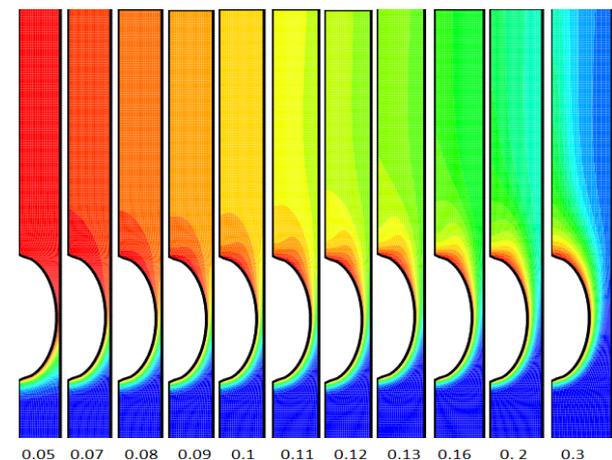
Figure 12. Temperature contour with various spacing between the tubes for (Ra=10^5, $Pr = 0.7$ and axis ratio ε= 0.25).
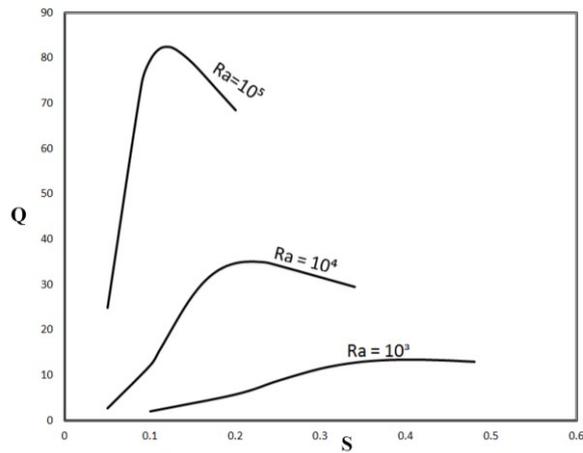
Figure 13. Heat transfer density with spacing at difference Rayleigh number for axis ratio ε=0.1.
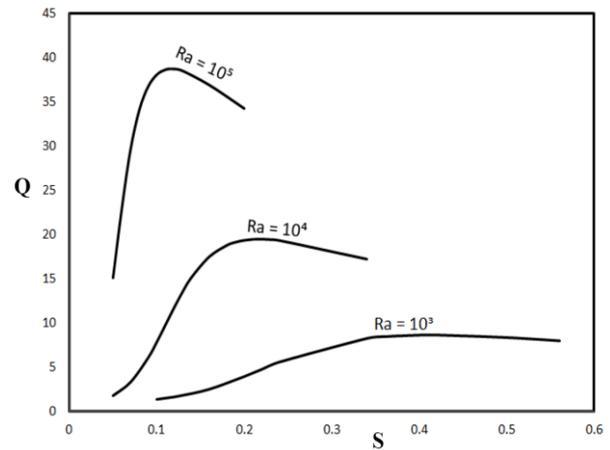
Figure 14. Heat transfer density with spacing at difference Rayleigh number for axis ratio ε=0.25.
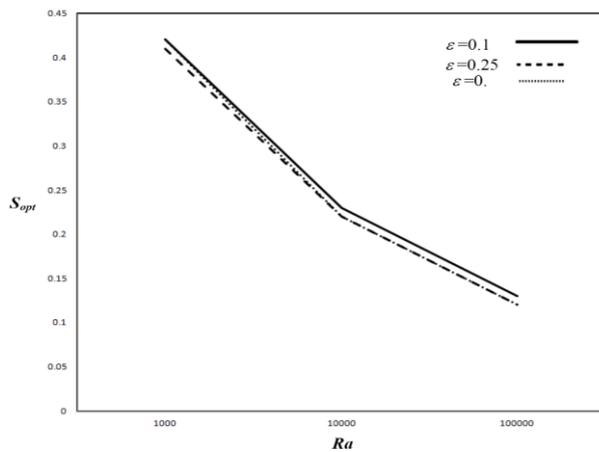
Figure 15. Optimum spacing with Rayleigh number of different axis Ratios.
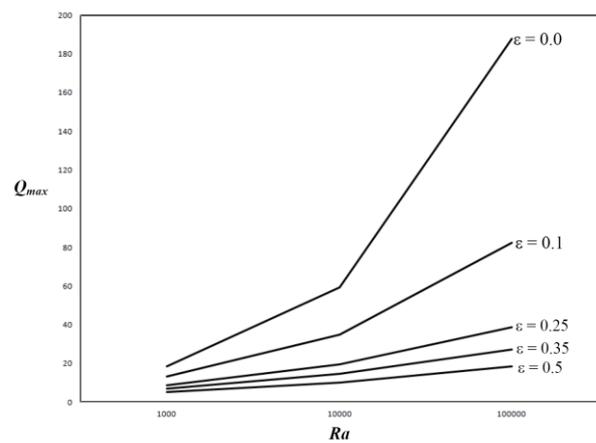
Figure 16. Maximum heat transfer density with Rayleigh number for different axis ratios.

7. Experimental results

Figure 18 shows the experimental heat transfer density (Q_{exp}) as a function of the spacing (S) between the tubes for ($Ra= 3.5\times 10^4$) and for axis ratio of ($\varepsilon = 0.25$). This figure demonstrates the existence of the optimal spacing (S_{opt}) that maximizes the heat transfer density. The behavior of the experimental curve is similar to the numerical curve of the heat transfer density with spacing which shown in Figure 12. The agreement between the experimental and numerical results is qualitative. Table 4 shows the comparison between the experimental heat transfer density and the numerical heat transfer density for Rayleigh number ($Ra = 3.5\times 10^4$) and axis ratio ($\varepsilon = 0.25$). The agreement between the experimental and numerical S_{opt} values (within maximum percentage error 37%) is reasonable in view of the by-pass air flow from the sides of the row. The limitation in the experimental apparatus is the horizontal dimension (L), in the experiment a buoyant air is by-passed on the outside of the elemental channels and this is differing from the numerical model in which assumed that ($L>>S$)(so that in numerical model the by-pass air from the row sides is negligible). In the view of the mentioned by-pass air the agreement between the experimental and numerical results is good.

Table 4. Comparison between numerical and experimental heat transfer density for (Ra = 3.5×10^4 and ε =0.25).

Case	$Q)num.$	$Q)exp.$	Error%
5 pipe	23.788	37.76	37
4 pipe	30.660	46.769	34
3 pipe	24.8744	38.837	36
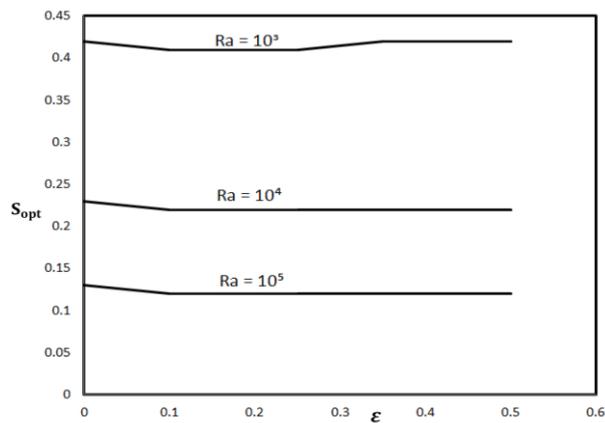
Figure 17. Optimum spacing with different axis ratios for Rayleigh Number.
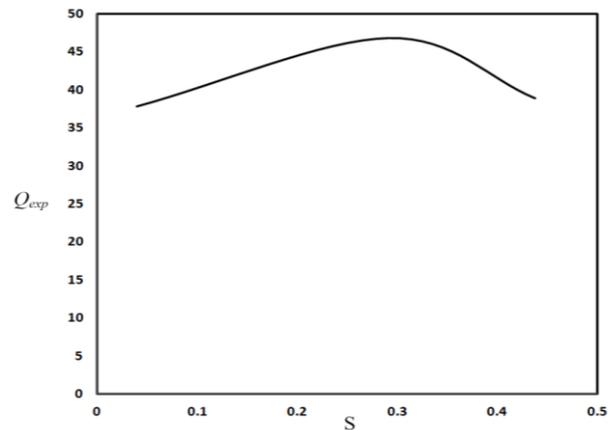
Figure 18. Experimental heat transfer density as a function of the spacing (S) between the tubes for ($Ra= 3.5 \times 10^4$) and ($\varepsilon = 0.25$).

8. Conclusions

The conclusions for optimal spacing between elliptic tubes cooled by natural convection can be summarized as:

1- The optimal spacing decreases as Rayleigh number increases for all axis ratios.
2- The maximum heat transfer increases as Rayleigh number increases for all axis ratios.
3- The highest value of the maximum heat transfer density occurs at axis ratio ($\varepsilon = 0$, flat plate) and lowest value occurs at axis ratio ($\varepsilon = 0.5$, circular plate) for all Rayleigh numbers.
4- The optimal spacing remains constant as the axis ratio increases at constant Rayleigh number.
5- The number of tubes installed in the same volume must be reduced as the axis ratio increases.
6- The agreement between the experimental and numerical heat transfer density is qualitative.

References

[1]   Bejan A., Lorente S. Design with Constructal Theory, Wiley, New York, 2008.
[2]   Bejan A. Convection Heat Transfer. Wiley, New York, 1984.
[3]   Bejan A. Fowler A.J., Stanescu G. The optimal spacing between horizontal cylinders in a fixed volume cooled by natural convection, International Journal of Heat and Mass Transfer 38, 2047-2055, 1995.
[4]   Ledezma G. A., Bejan A. Optimal Geometric Arrangement of Staggered Vertical Plates in Natural Convection, Journal of Heat Transfer, 119, 700-708, 1997.
[5]   Da Silva A.K., Bejan A. Maximal Heat Transfer Density in Vertical Morphing Channels with Natural Convection, Numerical Heat Transfer, Part A, 45: 135-152, 2004
[6]   Da Silva A.K., Bejan A. Constructal multi-scale structure for maximal heat transfer density in natural convection, Int. J. Heat Fluid Flow 26, 34-44, 2005.
[7]   Da Silva A.K., Lorenzini G., Bejan A. Distribution of heat sources in vertical open channels with natural convection, International Journal of Heat and Mass Transfer 48, 1462–1469, 2005.
[8]   Bello-Ochende T., Bejan A. Constructal multi-scale cylinders with natural convection, International Journal of Heat and Mass Transfer 48, 4300-4306, 2005.
[9]   Page L., Bello-Ochende T., Meyer J. Maximum heat transfer density rate enhancement from cylinders rotating in natural convection, Int. Commun. Heat Mass Transfer 38, 1354-1359, 2011.
[10]   Page L., Bello-Ochende T., Meyer J. Constructal multi scale cylinders with rotation cooled by natural convection, International Journal of Heat and Mass Transfer 57, 345-355, 2013.
[11]   Zhang Z., Bejan A., Lage J.L. Natural Convection in a Vertical Enclosure with Internal Permeable Screen, Journal of Heat Transfer, 113, 377-383, 1991.

[12]   Rhie, C. M., Chow, W. L. Numerical Study of the Turbulent Flow Past an Airfoil with Trailing Edge Separation, AIAA Journal, 21, 1525-1532, 1983.

Ahmed Waheed Mustafa, born in Baghdad –Iraq, 1976, and he received the B.S. and M.Sc. degrees in (Mechanical Engineering/ air conditioning and refrigeration) from university of technology in 1998 and 2001,respectively, and Ph.D in (Mechanical Engineering / Power)from Baghdad University in 2005. He is now assistant professor in Al-Nahrain University – College of Engineering –Mechanical Engineering Department.
E-mail address: ahmedwah@eng.nahrainuniv.edu.iq

Jafar Ahmed Zahi Researcher in Thermal Engineering Department of Mechanical Engineering, Al-Nahrain University, Iraq. He received the B.Sc. degree in Mechanical Engineering from the Collage of Engineering, University of Kufa, Iraq.
E-mail address: Jafaralkhafajy@gmail.com